A new heterogeneous catalytic system for wastewater treatment: Fe-immobilized polyelectrolyte microshells for accumulation and visible light-assisted photooxidative degradation of dye pollutants

Xia Tao [a,*], Jingmei Su [a], Lingxuan Wang [b], Jian-Feng Chen [c,*]

[a] Key Lab for Nanomaterials of the Ministry of Education, Beijing University of Chemical Technology, Beijing 100029, China
[b] Key Laboratory of Photochemistry, Institute of Chemistry, Chinese Academy of Sciences, Beijing 100080, China
[c] Research Center of the Ministry of Education for High Gravity Engineering & Technology,
Beijing University of Chemical Technology, Beijing 100029, China

Abstract

Fe-immobilized polyelectrolyte microshells have been successfully constructed by alternative adsorption of Fe(III) and alginate sodium (ALG) onto the precursor shells composed of chitosan (CHI) and ALG templated on melamine formaldehyde (MF) particles. Confocal laser scanning microscopy (CLSM) directly demonstrated that the as-synthesized $(ALG/CHI)_4(ALG/Fe)_n$ ($n = 1, 2$) shells could accumulate efficiently rhodamine B (RhB), methylene blue (MB) and acridine orange (AO) in well-defined internal space under moderate conditions via a simple mix processing. Further, H_2O_2 could cross the Fe-immobilized shell walls and react with the dyes concentrated in the interior of shells under visible radiation. The photodegradation of dyes accumulated in the microshells in the presence of H_2O_2 was characterized by UV–vis adsorption spectra and CLSM. More importantly, the photooxidative reaction occurring in the Fe-immobilized microshells can be performed at a wide range of pH from acid to neutral media, which is superior to the conventional Fenton reaction that allows taking effect only under acid condition of pH <4. Electron paramagnetic resonance (EPR) and other studies into the mechanism of the light-activated reaction process give tentative evidence that distinct from the photoreaction occurring in neutral medium, the photoreaction taking place in confined microshells in acid medium proceeds mainly through $HO^\bullet$ radicals with high oxidative potential.
© 2007 Elsevier B.V. All rights reserved.

*Keywords:* Dyes; Iron; Microshells; Photodegradation; Self-assembly

1. Introduction

Elimination of persistent and nonbiodegradable organic pollutants in water by oxidation with H_2O_2 has been studied extensively, in which the oxidant H_2O_2 could be activated catalytically by iron species such as iron porphyrin, iron phthalocyanine, and iron hydroxide [1–6]. To enhance the catalytic activity of the reaction system and the stability of the catalysts, these iron species are generally managed to bind on appropriate support materials such as neutral organic polymers, ion

exchange membranes or resins, and inorganic materials (clay, zeolites etc.) [7–10]. Further, another advantage of a supported catalyst system is the ease of separation from the reaction solution by filtration [11]. Zhao and coworkers described a novel catalytic system consisting of iron tetrasulfophenylporphyrin immobilized on a commercial anionic ion-exchange resin to activate H_2O_2 in aqueous media for the photodegradation of organic pollutants, especially for the degradation of anionic and non-ionic compounds [12]. Meunier and Sorokin reported that 2,4,6-trichorophenol in a mixed CH_3CN/H_2O solvent could be efficiently degraded in the presence of H_2O_2 and supported iron phthalocyaninesulfonate [13]. In these heterogeneous catalytic processes, active oxygen species with high oxidation activity, for example, hydroxyl radical, hydroperoxyl radical and/or high-valence iron complexes are involved [14–17]. Despite their
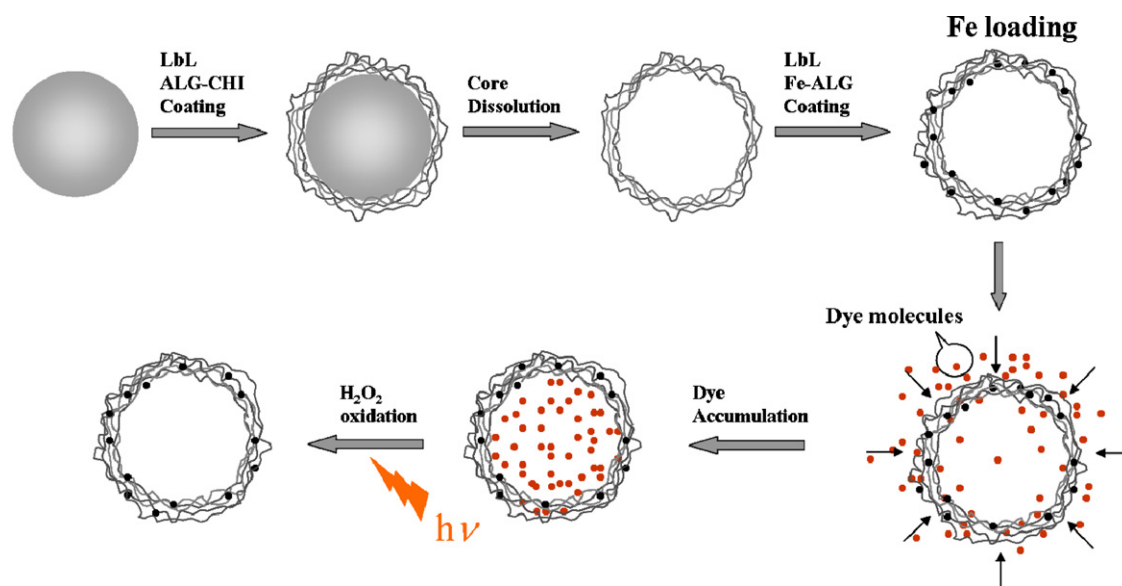
Scheme 1. Schematic illustration of the procedure for the visible light-assisted degradation of dye pollutants accumulated in the preformed Fe-immobilized polyelectrolytes microshells.

potential in pollution treatment, these systems could suffer from the drawback of an excessive loss of the generated active species with short life-time before reacting with organic pollutants with lower concentration levels. Therefore, developing a new system/device to utilize effectively the active oxygen species generated in the heterogeneous catalytic system containing immobilized iron species and H_2O_2 for the remediation of pollutants remains an important issue.

Tiny three-dimensional polyelectrolyte microshells have been successfully fabricated by using the layer-by-layer (LbL) assembly technique that relies on electrostatic coating of oppositely charged polyelectrolytes onto colloidal particles, followed by removal of the template cores [18]. The constructed LbL shells with well-controlled size and shape, finely tuned shell thickness, and variable wall compositions have been widely investigated in many practical applications such as drug delivery, catalysis, biomedicine and materials science [19–21]. However, to date, very few studies have been conducted that aims to use nano- and micro-sized shells as green microreactors for the environmental treatment of organic pollutants in water. In our recent work, we, based on the permeable property of the shells as well as spontaneous deposition of organic species in the shells, have described a novel route for the effective elimination of dye pollutants by introducing the assembled shells into dye-polluted systems [22]. We found that dye molecules can cross the shell wall barrier and then be accumulated inside the preformed microshells under moderate conditions. Combined with homogeneous Fenton reagent (Fe^{3+}/H_2O_2) the accumulated dyes in defined regions can be effectively degraded in aqueous media under visible radiation.

As a matter of fact, high-valence metal ions are facile to be assembled on the polyelectrolyte microshells by electrostatic LbL technique [23]. In this work we report the development of a photocatalytic treatment system by means of immobilizing iron ions onto the shell walls for the sake of avoiding little activ-

ity for substrate degradation due to the precipitation of the Fe ions at pH >4 as well as difficult post-treatment of Fe sludge after the reaction [24]. Herein, the Fe-immobilized polyelectrolyte microshells are constructed through electrostatic LbL self-assembly technique, in which natural polymers e.g. alginate sodium (ALG) and chitosan (CHI) along with perchloric acid iron are used as shell wall components (Scheme 1). Typically, the (ALG/CHI)$_4$/ALG shells were used as templates for the further LbL deposition of Fe. Rhodamine B (RhB), methylene blue (MB) and acridine orange (AO) are chosen as target pollutants to evaluate the loading capability and photostability of the Fe-immobilized shells. We find that the Fe-immobilized shells i.e. (Fe/ALG/CHI) shells can accumulate dyes efficiently in water under moderate conditions (room temperature, pure water medium) via a simple mix processing. Further, the accumulated dyes in the interior of shells were degraded at a rapid rate by H_2O_2 oxidation under visible light at a wide range of pH from acid to neutral suspension. Integrated spherical shape of the shells after the photoreaction was also discerned. An interesting finding is that the photoreaction in acid medium involves mainly the formation and reaction of HO$^\bullet$ radicals whereas in neutral medium no signals of HO$^\bullet$ radicals are detected. Based on spin-trapping EPR and other experimental results, possible accumulation and photoreaction process is also discussed in this work.

2. Experimental

2.1. Materials

ALG (Mw = 12,000–80,000) was obtained from Sigma, Canada. CHI (Mw = 30,000) was obtained from Primex Biochemicals, Norway. Melamine formaldehyde (MF) particles (4.31 ± 0.18 μm) were purchased from Microparticles GmbH, Germany. Ferric perchlorate (Fe(ClO$_4$)$_3$·6H$_2$O) was purchased

from Aldrich Chemical Co. RhB, MB and AO were of analytic reagent grade and used without further purification. The reagent 5,5-dimethyl-1-pyrroline-*N*-oxide (DMPO) used as the spin-trapping agent in EPR studies was purchased from Sigma Chemical Co. Superoxide dismutase (SOD) was purchased from Shijiazhuang pharmaceutical factory. All chemicals were used as received. Millipore water was used throughout the study. Unless otherwise noted, the pH of the photodegradation system was adjusted to 2.7 or 6.0 by diluted aqueous solutions of NaOH or $HClO_4$. For reference, the structures of RhB, MB and AO are shown below:
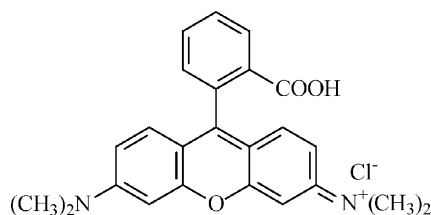
Rhodamine B (RhB)
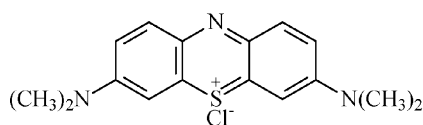
Methylene blue (MB)
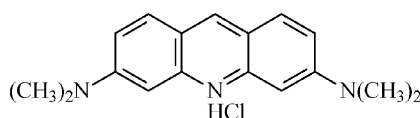
Acridine orange (AO)

2.2. Procedure for the assembly of Fe-immobilized and dye-accumulating microshells

1.5 ml of alginate solution (1 mg/ml in 0.5 M NaCl) or 1.5 ml of chitosan solution (1 mg/ml in 0.2 M NaCl at pH 3.8), with a charge opposite to that of MF templates (microparticles GmbH, Germany) or the last layer deposited, was added to a template colloidal solution (0.3 ml), and left to absorb for 1 h. The excess of added species was removed after each layer was deposited by three repeated centrifugation ($2500 \times g$, 3 min)/washing/redispersion cycles with dilute aqueous NaCl. After completing of $(ALG/CHI)_4$/ALG deposition, hollow microshells were obtained by dissolving the MF cores with HCl (0.1 M), centrifuging ($2500 \times g$, 5 min) and washing three times with water. Subsequent alternate adsorption of $Fe(ClO_4)_3$ (3×10^{-3} M, pH 2.5) and ALG was carried out by using a similar procedure, except that the Fe deposition was left overnight. The synthesized $(ALG/CHI)_4(ALG/Fe(III))_n$ ($n = 1, 2$) shells were labeled with Fe-she1 and Fe-she2, respectively. Fe-She2 was used in subsequent studies on the photocatalytic behavior of the accumulated dyes. All adsorption procedures were carried out at ambient temperature.

Equal amounts of a Fe-immobilized shell suspension and a dye solution were mixed together overnight. The filled shells were rinsed with Millipore water until no dye in the supernatant

solution was detected by UV–vis measurements. The final total volume is diluted to 4 ml for subsequent photoreaction.

2.3. Photoreactor and light source

A halogen lamp (Institute of Electric Light Source, Beijing) was positioned inside a cylindrical Pyrex vessel surrounded by a jacked with circulating water (Pyrex) to cool the lamp. A light filter was equipped to completely remove any radiation below 420 nm and to ensure illumination by visible light only.

2.4. Procedures and analyses

A drop of Fe-immobilized shell suspension was deposited and dried onto a Cu-grid. Transmission electron microscopy (TEM) images were recorded with JEM-3010 microscope operated at an acceleration voltage of 120 kV.

Confocal images were taken with by using an Olympus FV500 confocal laser scanning microscopy (CLSM) equipped with multiple laser lines for excitation of fluorophores. The CLSM images were acquired in aqueous environment. The optical parameters of the CLSM remained unchanged prior to and after the photoreaction so that the intensities obtained could be compared quantitatively.

Unless noted otherwise, all the irradiation experiments were carried out in a quartz cell with an appropriate stirrer. The temporal absorption spectra changes taking place during the photoreaction of dye-accumulated Fe/ALG/CHI shells with H_2O_2 under visible illumination were recorded using a UV2501 spectrophotometer (Shimazdu, Japan).

Electron Paramagnetic Resonance (EPR) signals of radicals spin-trapped by DMPO were recorded at ambient temperature on a Brucker EPR E500 spectrometer. The irradiation source was a Quanta-Ray Nd: YAG pulsed laser system ($\lambda = 532$ nm).
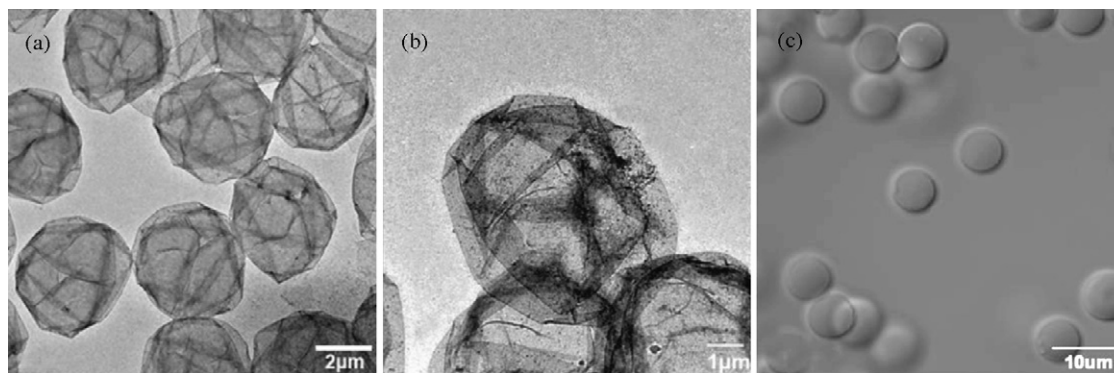
Fig. 1. TEM images of (ALG/CHI)$_5$ shells (a) and Fe-immobilized shells (b). (c) CLSM transmission image showing intact spherical shape of Fe-immobilized shells.

3. Results and discussion

3.1. Preparation of Fe-immobilized and dye-accumulating microshells

High-valence ions as building blocks can be incorporated into polyelectrolyte shell walls via stepwise LbL self-assembly process (see Section 2 for details). Here, Fe^{3+} and ALG as pairs are assembled on the preformed hollow (ALG/CHI)$_4$/ALG shells by electrostatic interaction of Fe^{3+} and carboxylic groups of ALG chains. Fig. 1a and b show typical TEM images of the ALG/CHI and Fe-immobilized ALG/CHI polyelectrolyte hollow shells fixed on Cu-grid and air drying. Clearly, compared with Fig. 1a, the dark phase observed in Fig. 1b is arisen from the Fe coating on shell walls. A CLSM transmission image shows that the constructed (Fe/ALG/CHI) microshells keep their spherical shape intact in a wet state (Fig. 1c). The loading amount of Fe on the shells was quantified by means of using a modified 1,10-phenanthroline method [25]. Two types of shells i.e. the (ALG/CHI)$_4$(ALG/Fe(III))$_n$ (n = 1, 2) shells abbreviated as Fe-She1 (n = 1) and Fe-She2 (n = 2) were constructed. By measurement, ca. 0.37×10^{-6} μmol/shell of the loading amount for Fe-She1 is obtained. Upon increasing the number of assemblies from the monolayered Fe-She1 to the dilayered Fe-She2, the loading amount of Fe doubles accord-

ingly, reaching to 0.74×10^{-6} μmol/shell. This suggests that the immobilizing amount of Fe on the shells can be controlled by the assembled number of layer.

The accumulation of dye in the Fe-immobilized hollow shells was performed by adding a solution of RhB, MB or AO to a suspension of the (Fe/ALG/CHI) shells overnight at ambient temperature. We find that RhB, MB and AO all can cross the (Fe/ALG/CHI) layer barrier easily, and then accumulate inside the shells. Compared with the adsorption bands of free dyes in aqueous solutions, the maximum absorption peak of all accumulated dyes in the microshells has a shift to some degree, suggesting the existence of aggregates of dyes in defined microenvironment. Additionally, CLSM images verified directly the efficient accumulation of RhB and MB in the interior of the (Fe/ALG/CHI) shells with almost complete integrity, yielding a higher concentration than in the bulk, as shown in Fig. 2. The accumulated amount of dye in a single shell composed of (Fe/ALG/CHI) is calculated as 0.08×10^{-6} μmol for RhB, 0.22×10^{-6} μmol for MB and 0.30×10^{-6} μmol for AO, as summarized in Table 1.

3.2. Photocatalytic behavior of dyes in the shells

After simple separation by filtration, the dye-accumulating (Fe/ALG/CHI) microshells were dispersed in H_2O_2 solution.
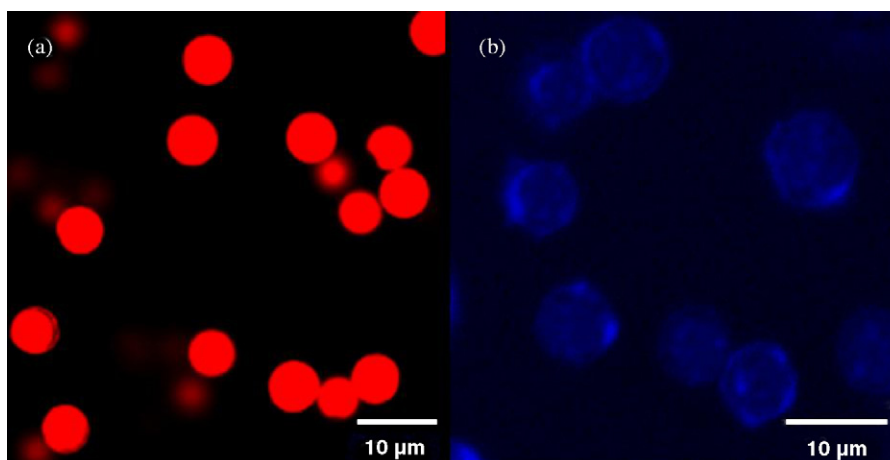

Fig. 2. CLSM images of the Fe-immobilized shells accumulating RhB (a) and MB (b).

Table 1
Loading behavior of dyes in the hollow Fe-She2 shells[a]

Dye	Amount of dyes added (μmol)	Loading amount of dyes ($\times 10^{-6}$ μmol/shell)
RhB	0.06	0.08
MB	0.12	0.22
AO	0.16	0.30

[a] In each experiment, 30 mg of MF particles were used to fabricate the shells, which corresponds to ∼0.5 million of preformed shells. The loading amount of dyes on shells could be determined by the difference between the initial concentration of dyes added and the amount of non-accumulated dyes remaining in the supernatant liquid, combined with their respective standard curves.

The changes in UV–vis spectra of accumulated RhB, MB and AO in the presence of H_2O_2 under visible light irradiation at pH 2.7 were shown in Fig. 3. The characteristic absorption band of RhB at 556 nm decreased rapidly with increasing visible irradiation time, and disappeared ultimately after 90 min of irradiation (Fig. 3a). A control experiment showed that no significant changes of accumulated RhB absorption spectra were observed in the dark compared to the photoreaction, suggesting that visible illumination accelerated markedly the degradation process. Similarly, we carried out the experiments on the photoreaction of MB and AO under the same experimental condition as Fig. 3a. It was found that the characteristic absorption band of MB and AO accumulated inside the shells also disappeared rapidly after irradiation for 80 min and 70 min, respectively (Fig. 3b and c). These indicated that under current condition at least the chromophoric structure of the dyes accumulated inside the (Fe/ALG/CHI) shells was subject to the destruction.

Direct visualization on the changes in the accumulated RhB or MB inside the (Fe/ALG/CHI) shells before and after the photoreaction was also traced by CLSM measurements. Fig. 4 displays CLSM images of the RhB-accumulated (Fe/ALG/CHI) shells in H_2O_2 before and after exposure to visible radiation for 0, 60 and 120 min, respectively. Apparently, the fluorescence intensity of the shell interior (proportional to the accumulated RhB concentration) reduces at a rapid rate with increasing radiation time. In addition, we used CLSM to examine the photodecoloration of the accumulated MB inside the Fe-immobilized shells in H_2O_2 solution (Fig. 5). Since the fluorescence intensity of the MB-accumulating shells after the photoreaction for 100 min was extremely weak just as Fig. 4c, a transmission image (Fig. 5b) instead of a fluorescence image is displayed. This result also suggests that the accumulated MB in the (Fe/ALG/CHI) shells can be photodecolored at a rapid rate in the presence of H_2O_2 at pH 2.7. Furthermore, one can see that RhB or MB molecules are located well in the interior of the shells due to no fluorescence in the bulk solution in the course of photoreaction. It should also be pointed out that the (Fe/ALG/CHI) shells still keep their spherical shape during the photoreaction, indicating that the assembled (Fe/ALG/CHI) shells are stable against attack from highly active species emanated from the heterogeneous photo-oxidative reaction occurring in restricted spaces.

More interestingly, the constructed (Fe/ALG/CHI) shells can not only efficiently accumulate the dye molecules entering into
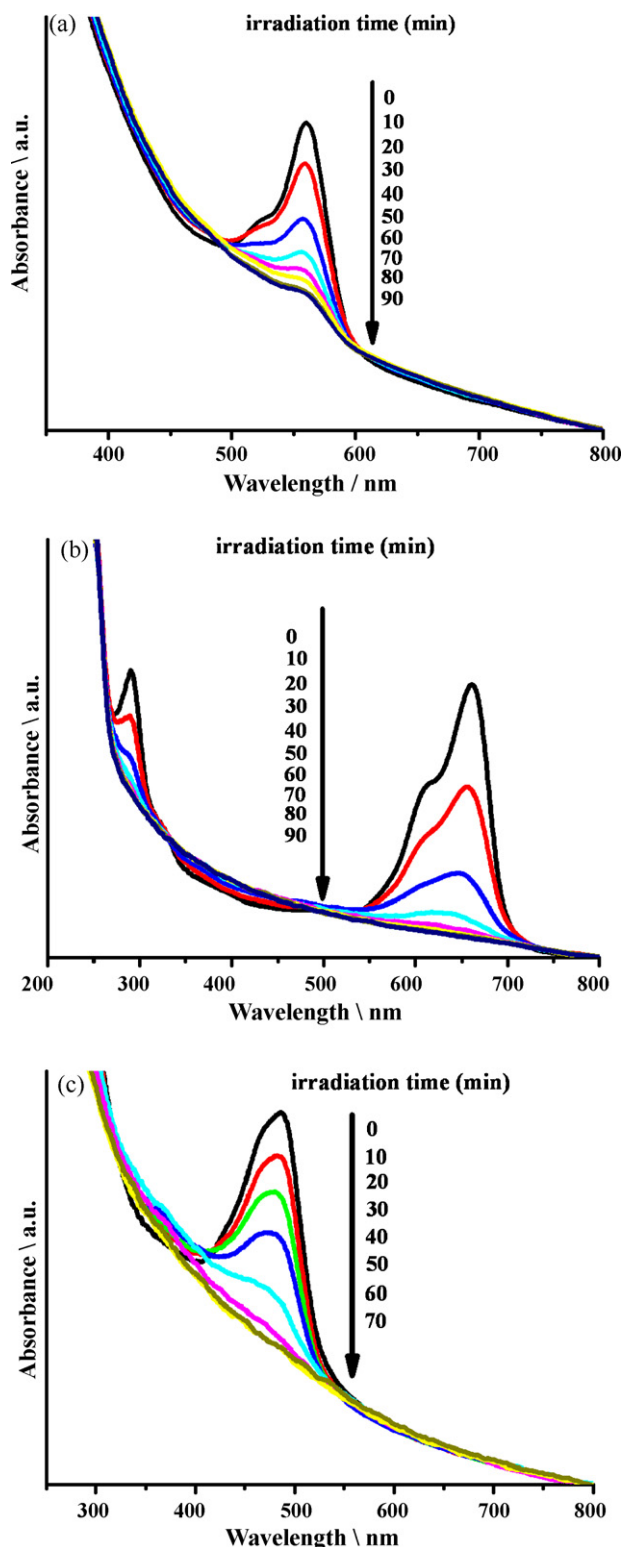

Fig. 3. UV–vis spectral changes of accumulated (a) RhB (10 μM), (b) MB (27 μM), (c) AO (36 μM), in the presence of Fe-She2 (0.1 mM) and H_2O_2 (0.75 mM) under visible irradiation, pH: 2.7.

the shells under ordinary conditions, but extend the coverage of homogenous Fenton reagent (Fe^{3+}/H_2O_2) to neutral media as well. Fig. 6 displays the changes that took place to the temporal absorption spectra of dyes accumulated inside the
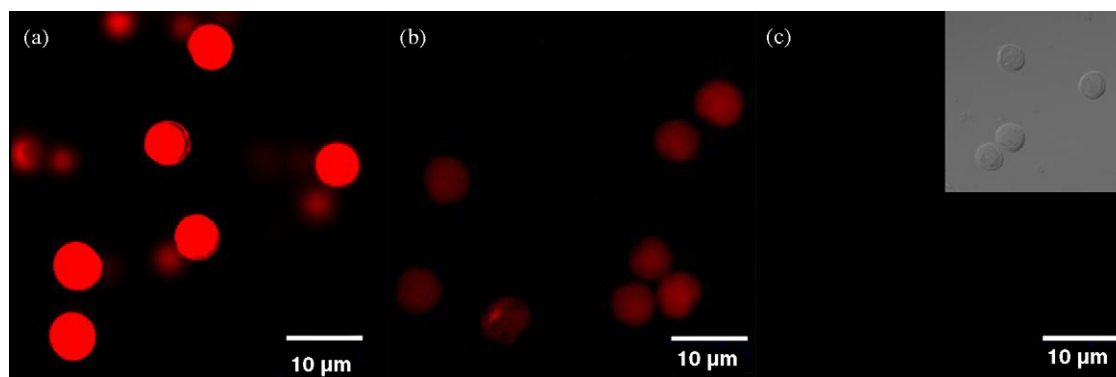
Fig. 4. Variations in CLSM fluorescence images of Fe-immobilized shells accumulated with RhB in the presence of H_2O_2 (0.75 mM) before (a) and after irradiation for 60 min (b) and 120 min (c), respectively. During the measurements the optical parameters of the CLSM remained unchanged. Inset in (c) shows CLSM transmission image of the RhB-accumulated shells under the same condition as (c). Photoreaction proceeds in an aqueous solution of pH 2.7.

(Fe/ALG/CHI) shells in the presence of H_2O_2 under visible illumination at pH 6.0. Obviously, the characteristic absorption band of accumulated RhB and AO in visible region decreased rapidly. Besides, the photoreaction process in neutral media was also measured by CLSM, and the results show that during the whole photoreaction the (Fe/ALG/CHI) shells maintain their shape integral and the photoreaction takes place only in defined microshells.

The comparative studies for the photoreaction rate of dyes accumulated in the (Fe/ALG/CHI) shells in two sets of conditions i.e. acid and neutral media were shown in Fig. 7. For RhB system, in the first 40 min of photoreaction, ca. 80% of accumulated RhB was decomposed in an acid aqueous solution, whereas ca. 41% of accumulated RhB was decomposed in a neutral solution. Furthermore, the radiation time for complete decomposition of RhB is observed as 90 min in an acid solution and 140 min in a neutral solution. Likewise, for AO system, the radiation time for complete decomposition of AO is about 70 min in an acid solution and about 120 min in a neutral solution. Obviously, the photoreaction rate of accumulated dyes in both media is not uniform, which might be explained through active oxy-

gen species predominantly participated in the photoreaction (see vide post).

Additionally, we measured the total amount of iron ions present in the bulk solution after the photoreaction, and found that no significant amount of Fe was detected in the supernatant liquid. This means that Fe are closely attached, in a stable way, to the (ALG/CHI) shells, and thus leading to the Fe/ALG/CHI shells applicable in repetitive use.

3.3. Accumulation and photocatalytic mechanism discussion

As above-mentioned in Fig. 2, the loading amount of dyes in the (Fe/ALG/CHI) shells is ~10^{-7} μmol/shell, which is comparable to that of dyes in the (ALG/CHI) shells [22]. This indicates the immobilization of iron on the shells has no little influence on the accumulation amount of dyes; in other word, the accumulation amount of dyes in the shells is mainly attributed to the nature of internal layer of the shells themselves. Furthermore, the accumulated dyes might be more likely to be in an aggregated or complex form so that the
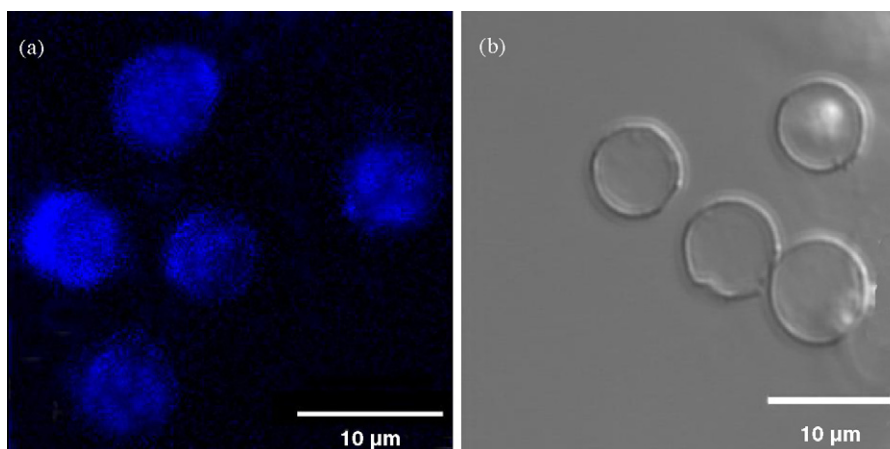

Fig. 5. CLSM images of Fe-immobilized shells accumulated MB (27 μM) in the presence of H_2O_2 (0.75 mM) before (a) and after irradiation for 100 min (b). Reaction solution is adjusted to pH 2.7. Note: fluorescence image (a); transmission image (b).
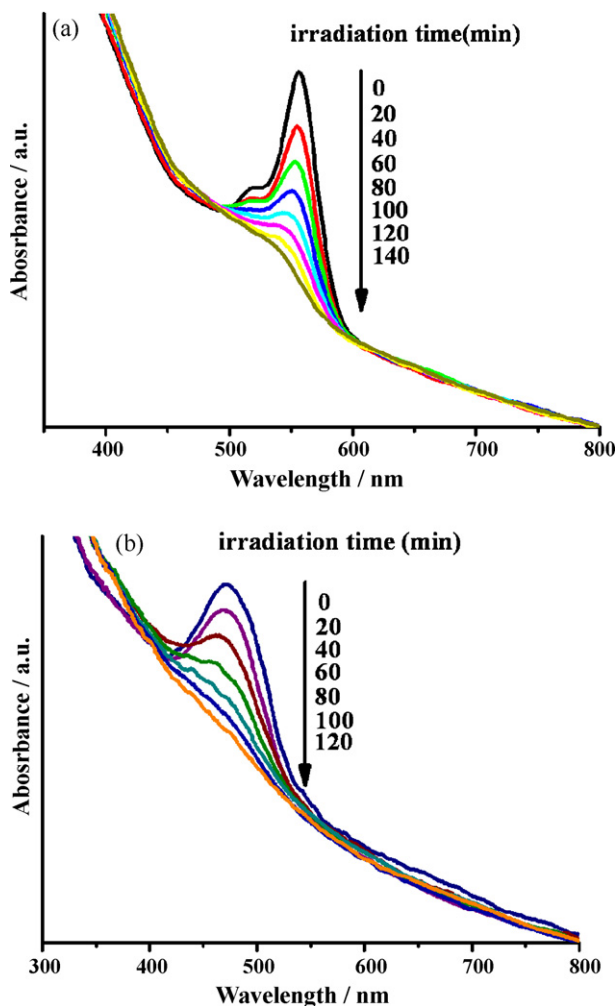
Fig. 7. Photoreaction rate of accumulated dyes in two sets of conditions (a) RhB, pH 2.7; (b) AO, pH 2.7; (c) RhB, pH 6.0 and (d) AO, pH 6.0.

Fig. 6. UV–vis spectral changes of accumulated RhB (10 μM) (a) and AO (36 μM) (b) in the presence of Fe-She2 (0.1 mM) and H_2O_2 (0.75 mM) under visible irradiation, pH 6.0.

real concentration within the interior of the microshells is lower than in the bulk solution, thus promoting accumulation [25].

To gain more insight into the nature of short-lived radicals formed during the photoreaction under visible irradiation in two different media, spin-trapping ESR technique was used (Fig. 8). When the reaction system is in an acid solution, no
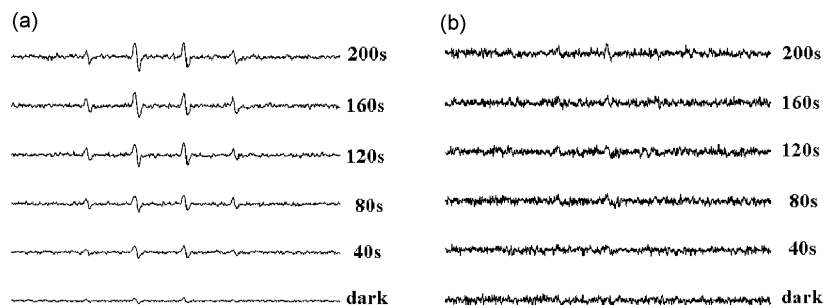
signals with a significant intensity in the dark were observed, whereas upon 532 nm laser irradiation the characteristic quartet peaks of DMPO-HO$^\bullet$ (DMPO = 5,5-dimethyl-1-pyrroline-N-oxide) adducts with an intensity of 1:2:2:1 appeared and increased gradually with laser radiation (Fig. 8a). This is consistent with similar spectra reported by others for HO$^\bullet$ adducts [26] and this indicates that HO$^\bullet$ radicals are generated and participated in the photoreaction of RhB accumulated in the (Fe/ALG/CHI) shells in an acid medium. In another experiment, it was found that the addition of ethanol, a known scavenger of HO$^\bullet$ radicals, to the photoreaction system markedly retarded the photooxidative reaction rate of RhB accumulated in the shells in an acid medium, and this further verified that HO$^\bullet$ radicals are involved in the photoreaction process [27]. When dispersing the RhB-accumulating (Fe/ALG/CHI) microshells in a neutral solution with H_2O_2 presence, no signals were detected whether in the photoreaction or in the dark (Fig. 8b). This indicates that the photoreaction process in a neutral medium might not be mainly HO$^\bullet$ radical-dependent. Besides, the addition of superoxide dismatase (SOD) arose apparent changes to adsorption curve profile of the accumulated RhB or AO, suggesting that $^\bullet$OOH/$O_2^{\bullet-}$ radicals as active oxygen intermediates might be involved in the reaction process. In such case, the faster photoreaction rate of dyes defined in the microspace in an acid solution than in a neutral solution might be ascribed to higher oxidative activity of HO$^\bullet$ radicals than that of $^\bullet$OOH/$O_2^{\bullet-}$ radicals involved in

Fig. 8. Changes in the EPR signals of solutions containing RhB (10 μM), Fe(III) (0.1 mM) and H_2O_2 (0.75 mM), measured both in the acid solution of pH 2.7 (a) and in the neutral solution of pH 6.0 (b). The 1:2:2:1 quartet peak is due to the DMPO-HO$^\bullet$ adducts formed.
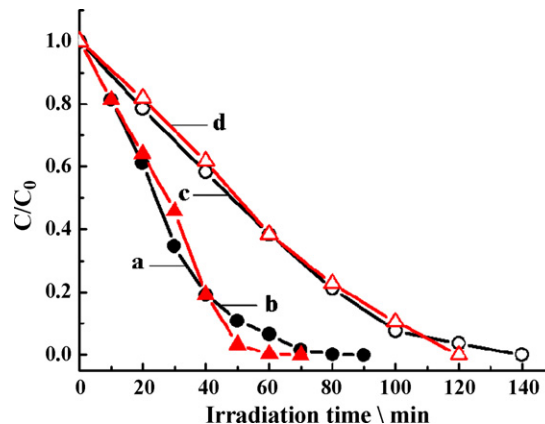
the photoreaction studied (see Fig. 7) [26–28]. Further study is needed for the detailed photoreaction mechanism.

4. Conclusion

We have successfully constructed Fe-immobilized polyelectrolyte microshells through the LbL self-assembly technique. The resulting shells have been verified to be effective in the accumulation of dye pollutants in water and subsequent visible light-assisted degradation by H_2O_2 oxidation. The stable performance and the accumulating capacity to organic species of the Fe-immobilized polyelectrolyte microshells not only might open perspectives for the economical treatment of dye pollutants in natural aqueous ecosystems but also is useful for a better understanding of the visible light-assisted heterogeneous catalytic mechanism occurring in defined microspace.

Acknowledgements

References

[1] (a) A. Sorokin, J.L. Seris, B. Meunier, Science 268 (1995) 1163–1166;
(b) G. Labat, J.L. Seris, B. Meunier, Angew. Chem. Int. Ed. 29 (1990) 1471–1473.

[2] (a) T.J. Collins, Acc. Chem. Res. 35 (2002) 782–790;
(b) C.G. Miller, S.W. Gordon-Wylie, C.P. Horwitz, S.A. Strazisar, D.K. Per, G.R. Clark, S.T. Weintraub, T.J. Collins, J. Am. Chem. Soc. 120 (1998) 11540–11541;
(c) S.S. Gupta, M. Stadler, C.A. Noser, A. Ghosh, B. Steinhoff, D. Lenoir, C.P. Horwitz, K.W. Schramm, T.J. Collins, Science 296 (2002) 326–328.

[3] (a) X. Tao, W. Ma, T.Y. Zhang, J. Zhao, Angew. Chem. Int. Ed. 40 (2001) 3014–3016;
(b) X. Tao, W. Ma, T.Y. Zhang, J. Zhao, Chem. Eur. J. 8 (2002) 1321–1326.

[4] (a) H. Wariishi, M. Kabuto, J. Mikuni, M. Oyadomari, H. Tanaka, Biotechnol. Prog. 18 (2002) 36–42;
(b) C.E. MacBeth, A.P. Golombek, V.G. Young Jr., C. Yang, K. Kuczera, M.P. Hendrich, A.S. Borovik, Science 289 (2000) 938–941.

[5] (a) Y. Huang, J. Li, W. Ma, M. Chen, J. Zhao, J. Yu, J. Phys. Chem. B 108 (2004) 7263–7270;
(b) W. Ma, J. Li, X. Tao, J. He, Y. Xu, J. Yu, J. Zhao, Angew. Chem. Int. Ed. 42 (2003) 1029–1031.

[6] R.F. Parton, I.F.J. Vankelecom, M.J.A. Casselman, C.P. Bezoukhanova, J.B. Uytterhoeven, P.A. Jacobs, Nature 370 (1994) 541–544.

[7] M. Noorjahan, V. Durga Kumari, M. Subrahmanyam, L. Panda, Appl. Catal. B: Environ. 57 (2005) 291–298.

[8] A. Bozzi, T. Yuranova, J. Mielczarski, A. Lopez, J. Kiwi, Chem. Commun. (2002) 2202–2203.

[9] J. Li, W. Ma, Y. Huang, X. Tao, J. Zhao, Y. Xu, Appl. Catal. B: Environ. 48 (2004) 17–24.

[10] X. Tao, W. Ma, J. Li, Y. Huang, J. Zhao, J. Yu, Chem. Commun. (2003) 80–81.

[11] D.J. Cole-Hamilton, Science 299 (2003) 1702–1706.

[12] Y. Huang, J. Li, W. Ma, M. Chen, J. Zhao, J. Phys. Chem. 108 (2004) 7263–7270.

[13] B. Meunier, A. Sorokin, Acc. Chem. Res. 30 (1997) 470–476.

[14] D.T. Sawyer, J.S. Valentine, Acc. Chem. Res. 14 (1981) 393–400.

[15] J. Kiwi, A. Lopez, V. Nadtochenko, Environ. Sci. Technol. 34 (2000) 2162–2168.

[16] C. Walling, Acc. Chem. Res. 8 (1975) 125–131.

[17] F. Chen, W. Ma, J. He, J. Zhao, J. Phys. Chem. A 106 (2002) 9485–9490.

[18] (a) Z. Dai, H. Möhwald, Chem. Eur. J. 8 (2002) 4751–4755;
(b) Z. Dai, L. Dähne, H. Möhwald, B. Tiersch, Angew. Chem. Int. Ed. 41 (2002) 4019–4022.

[19] A.D. Dinsmore, M.F. Hsu, M.G. Nikolaides, M. Marquez, A.R. Bausch, D.A. Weitz, Science 298 (2002) 1006–1009.

[20] (a) X. Qiu, S. Leporatti, E. Donath, H. Möhwald, Langmuir 17 (2001) 5375–5380;
(b) X. Tao, J. Li, H. Möhwald, Chem. Eur. J. 10 (2004) 3397–3403.

[21] (a) E. Saxon, C.R. Bertozzi, Science 287 (2000) 2007–2010;
(b) G.C.L. Wong, J.X. Tang, A. Lin, Y. Li, P.A. Janmey, C.R. Safinya, Science 288 (2000) 2035–2039;
(d) J. Locklin, K. Shinbo, K. Onishi, F. Kaneko, Z. Bao, R.C. Advincula, Chem. Mater. 15 (2003) 1404–1412.

[22] (a) X. Tao, J. Su, J.-F. Chen, J. Zhao, Chem. Commun. (2005) 4607–4609;
(b) X. Tao, J. Su, J.-F. Chen, Chem. Eur. J. 12 (2006) 4164–4169.

[23] I.L. Radtchenko, G.B. Sukhorukov, S. Leporatti, G.B. Khomutov, E. Donath, H. Möhwald, J. Colloid Interface Sci. 230 (2000) 272–280.

[24] (a) J. Feng, X. Xu, P.L Yue, Environ. Sci. Technol. 38 (2004) 269–275;
(b) J. He, X. Tao, W. Ma, J. Zhao. Chem. Lett. (2002) 86–87.

[25] X. Tao, X.-J. Sun, J. Su, J.-F. Chen, W. Roa, Polymer 47 (2006) 6167–6171.

[26] W. Song, W. Ma, J. Ma, C. Chen, J. Zhao, Environ. Sci. Technol. 39 (2005) 3121–3127.

[27] C. Kormann, D.W. Bahnemann, M. Hoffmann, Environ. Sci. Technol. 22 (1998) 998–1004.

[28] L. Weber, R. Hommel, J. Behling, G. Haufe, H. Hennig, J. Am. Chem. Soc. 116 (1994) 2400–2408.